Journal of Applied Polymer Science

Poly(ethylene terephthalate)/Poly(ethylene glycol-*co*-1,3/1,4-cyclohexanedimethanol terephthalate)/Clay Nanocomposites: Morphology and Isothermal Crystallization Kinetics

Jyh-Horng Wu,[1] Ming-Shien Yen,[2] M. C. Kuo,[2] Chien-Pang Wu,[1] Ming-Tsong Leu,[1] Chia-Hao Li,[1] F. K. Tsai[2]

[1]Nanomaterials Center, Industrial Technology Research Institute, Tainan 70955, Taiwan, Republic of China
[2]Department of Materials Engineering, Kun Shan University, Tainan 71003, Taiwan, Republic of China
Correspondence to: M. C. Kuo (E-mail: muchen@mail.ksu.edu.tw)

ABSTRACT: This work prepared poly(ethylene terephthalate)/clay (PET/clay), PET/poly(ethylene glycol-*co*-1,3/1,4-cyclohexanedimethanol terephthalate) (PET/PETG), and PET/PETG/clay nanocomposites via the twin-screw extrusion process. The organoclay in PET and PET/PETG matrices are in homogeneous dispersion, and the spacing distances between the platelets in the PET/clay and PET/PETG/clay nanocomposites are larger than 33.9 Å. Differential scanning calorimetry (DSC) and polarizing optical microscope (POM) analyses showed that the inclusion of organoclay significantly increased the crystallinities and melting temperatures of PET/clay and PET/PETG/clay nanocomposites with less time required to undergo isothermal crystallization. These findings imply the occurrence of heterogeneous nucleation. However, amorphous PETG substantially decreased the crystallinity of the crystallizable units of PET. Morphologically, the inclusion of organoclay drove the crystallites of PET from a spherulite with more perfection and less dimension to a larger spherulite. This process was extended from PET/clay to PET/PETG/clay in which the crystallites propagated in two-dimensional and disc-like morphology. However, blending PET with amorphous PETG imparted the larger crystallites with relatively distorted Maltese-cross patterns. © 2012 Wiley Periodicals, Inc. J. Appl. Polym. Sci. 000: 000–000, 2012

KEYWORDS: PET; PETG; clay; isothermal crystallization

Received 11 June 2012; accepted 13 June 2012; published online
DOI: 10.1002/app.38203

INTRODUCTION

PET is a semicrystalline engineering thermoplastic and widely used in textiles, automobiles, and food and beverage packaging. Apart from its high-performance mechanical properties and film clarity, the excellent gas-barrier property for reducing air permeability makes PET polymer an outstanding and unique material in food and beverage packaging applications. Understandably, PET has a worldwide consumption, second only to polyolefines. Recently, several researchers have reported that the incorporation of clay increases the gas barrier properties of PET/clay nanocomposites.[1–5] Nevertheless, the crystallization rate of PET/clay nanocomposites exceeds that of PET, in which the clay is believed to act as a nucleating agent.[6–17] PET/clay nanocomposites are generally opaque due to high crystallinity arisen by the inclusion of clay, and under this condition the nanocomposites can no longer be used in food and beverage packaging.

In contrast to semicrystalline PET polymers, PETG is an amorphous thermoplastic of the commercial PET family, with physical properties similar to PET.[18,19] In our previous study, we demonstrated that the amorphous nature of PETG would be unaffected by the inclusion of clay.[20] Instead, PETG has been found to form a miscible blend with PET.[21] Papadopoulou and Kalfoglou reported that the PET/PETG blend has a single endothermic peak in both T_g (93.3°C) and T_m (235.0°C) at a mixing ratio of 50/50 under the second heating run, indicating that this blend has good compatibility.[21] Moreover, the same researchers reported that PETG combines good toughness, even at low temperatures, with film clarity and melt strength. To improve the barrier properties of PETG polymer while maintaining its transparency, a nanocomposite of PETG/clay could be an approach for developing these novel materials.

The PET/PETG blend is one such crystalline/amorphous polymer blend. Blending PET with PETG is expected to reduce the crystallization rate of PET. As Papadopoulou and Kalfoglou reported that both the crystallinity and the melting temperature of neat PET can be lowered by blending PET with amorphous PETG.[21] However, the nucleation effect caused by clay would

Table I. Recipes for the Preparation of PET/PETG/Clay Nanocomposites, phr

Composition	PET	PETG	clay
PET	100	-	-
PETG	-	100	-
PET/PETG	50	50	-
PET/clay[a]	100	-	6
PETG/clay [a]	-	100	6
PET/PETG/clay[a]	50	50	6

[a]The clay was mixed with different aspect ratio of Closite 15A and MPGN in 1 : 1 weight ratio.

speed up and heighten the crystallization rate and the crystallinity of PET/clay nanocomposites compared to those of neat PET.[6,7] As stated previous, inclusion of clay would increase the crystallization rate, crystallinity, and gas barrier property but make PET opaque. Blending PETG with neat PET or PET/clay might reduce the crystallization rate and crystallinity of PET or PET/clay; as a result, it could maintain the transparency of neat PET. To achieve these attractive properties, basic studies on the PET/PETG/clay nanocomposites are continuously required. The objective of this study was to investigate the morphology and isothermal crystallization kinetics of PET/PETG/clay nanocomposites.

EXPERIMENTAL

Materials

The PET polymer (SHINPET 5015W) was kindly supplied by Shinkong Synthetic Fibers, Taiwan. PETG was prepared by two-stage melt-polycondensation (esterification and polycondensation) in an autoclave reactor. The molar ratio of ethylene glycol (EG)/1,3/1,4-cyclohexanedimethanol (1,3/1,4-CHDM) was 70/30. The details of the synthesis can be found in our previous study.[22] Closite 15A clay (aspect ratio 75–100) was obtained from Southern Clay. This clay had been treated with dimethyl dihydrogenated tallow quaternary ammonium chloride.

Sample Preparation

PET and PETG were molten and blended with clay (Table I) in a twin-screw extruder (Werner and Pflederer, Model-ZSK 26 MEGAcompounder) with corotating and intermeshing in 26 mm and *L/D* ratio of 56. The PET/clay and PET/PETG/clay nanocomposites were fabricated at a barrel temperature of 230–260°C and a screw speed of 500 rpm. The extruded strands were palletized and dried at 70°C for about 24 h.

TEM Observations

A HITACHI H7500 transmission electron microscope (TEM) was used to evaluate the dispersion condition of clay. The thin foil TEM specimens were prepared by microtome with a diamond knife, and examined in TEM operated at 120 kV.

XRD Measurements

X-ray diffraction (XRD) measurements were conducted on a Rigaku D/Max RC X-ray diffractometer using CuK_α radiation ($\lambda = 1.5418$ Å) at 40 kV and 100 mA with a scanning rate of 2° min^{-1}.

DSC Measurement

A TA differential scanning calorimeter (TA Q2000) was applied to investigate the isothermal crystallization behaviors of neat PET, PET/clay, PET/PETG, and PET/PETG/clay. The sample was heated up to 300°C at a rate of 10°C/min under nitrogen atmosphere. At 300°C, this sample was held for 3 min to remove the previous thermal history, and then it was quenched to the predetermined temperatures to undergo isothermal crystallization process. After the isothermal crystallization process, the sample was subsequently heated to 280°C to conduct the second heating run and to estimate the melting temperature (T_m).

POM Observations

A Nikon Optiphot-Pol universal stage polarizing optical microscope (Tokyo, Japan) was used to observe the spherulite morphologies of neat PET, PET/clay, PET/PETG, and PET/PETG/clay under isothermal crystallization. A thin piece of sample was sandwiched between two glass coverslips and placed on a digital hot-stage under nitrogen atmosphere. The hot-stage was rapidly heated to 300°C and held for 3 min to erase the thermal history of specimens. Then, the neat PET, PET/clay, PET/PETG, and PET/PETG/clay melts were quenched to the predetermined crystallization temperatures and kept at these temperatures for observations.

RESULTS AND DISCUSSION

TEM Observations

Figure 1 shows the distribution of the clay in the polymer matrices. The organoclay in these polymer matrices seems to be in homogeneous dispersion, indicating that the exfoliation or intercalation morphology of clay in the polymer matrices would be possible. Because of this homogeneous dispersion and the nano-sized dispersion domains, a investigation of crystallization kinetics under isothermal conditions is feasible.

XRD Analysis

Figure 2 shows the X-ray diffraction patterns for clay, PET/clay, PETG/clay, and PET/PETG/clay. The diffraction peaks at $2\theta = 2.370° \sim 2.555°$ are the characteristic diffraction of the (001) plane of Closite 15A clay. Accordingly, the *d*-spacings for Closite 15A, PET/clay, PETG/clay, and PET/PETG/clay are 37.11, 37.27, 36.12, and 34.58 Å, respectively. The *d*-spacings in the PETG containing nanocomposites are slightly lower than that of the PET/clay system, implying that the dispersion of the clay in the PETG containing nanocomposites might tend to allow more intercalation distributions.[7] The XRD results are consistent with the TEM observations, that is, the dispersion of organoclay in these polymer matrices is in homogeneous dispersion.

Regarding the effect of inclusion of clay on the crystal structure of PET or PET/PETG blend, we conducted the XRD analysis from $2\theta = 10° \sim 40°$, as shown in Figure 3. All the samples (PET, PET/clay, and PET/PETG/clay) exhibited the same diffraction peaks over the entire range of scans, which indicated that the inclusion of clay did not affect the crystal structure of PET polymer. The crystal structure of PET is a well known triclinic unit cell.[23] The PET/PETG (50/50) blend would significantly decrease the intensities at all the diffraction peaks, indicating that blending PET with PETG would suppress the crystallization behavior of neat PET polymer.

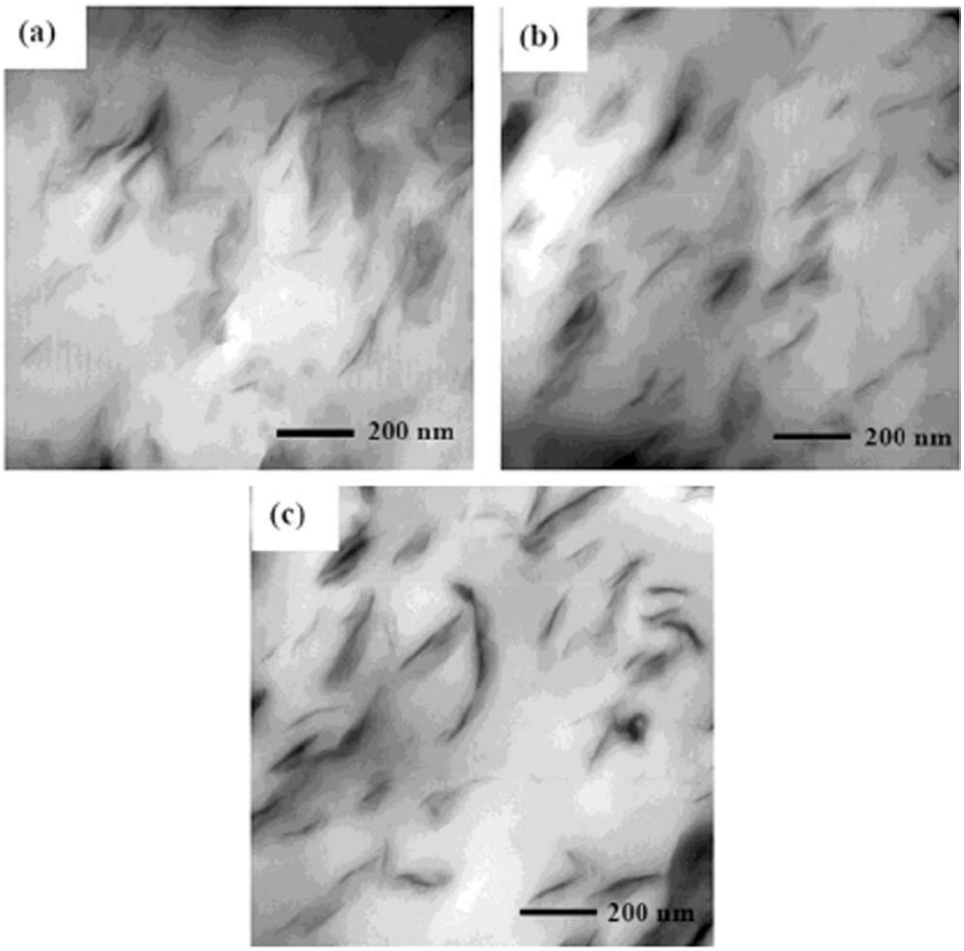

Figure 1. TEM micrographs showing the distribution of the organoclay in the polymer matrices: (a) PET/clay, (b) PETG/clay, and (c) PET/PETG/clay.

Isothermal Crystallization Behavior

Figure 4 shows the DSC isothermal crystallization traces of neat PET, PET/clay, PET/PETG, and PET/PETG/clay at the selected temperature intervals. The inclusion of clay could significantly raise the crystallization temperature intervals for both neat PET and PET/PETG blend. In contrast, this study hypothesized that blending PET with PETG would substantially suppress the crystallization behavior of PET because of the amorphous nature of

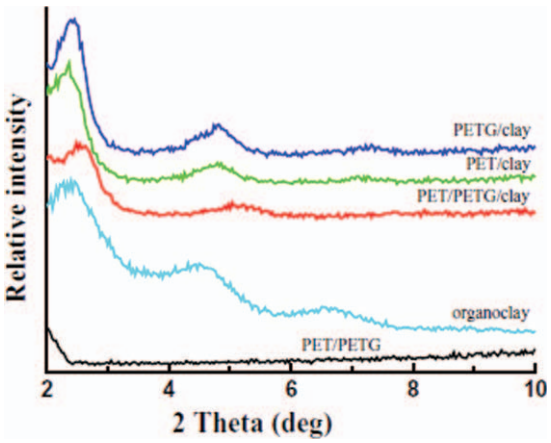

Figure 2. X-ray diffraction patterns of organoclay, PET/clay, PETG/clay, PET/PETG, and PET/PETG/clay. [Color figure can be viewed in the online issue, which is available at wileyonlinelibrary.com.]

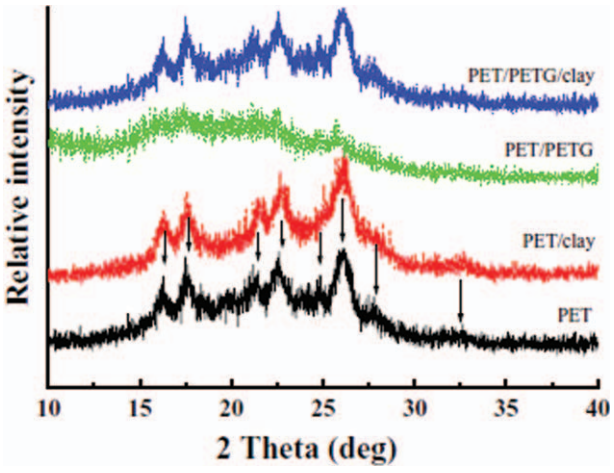

Figure 3. X-ray diffraction patterns of PET, PET/clay, PET/PETG, and PET/PETG/clay. As arrowed, the diffraction peaks at $2\theta = 16.24$, 17.47, 21.26, 22.59, 24.84, 27.80, and 32.61 are the zone planes of $(01\bar{1})$, (010), $(\bar{1}11)$, $(1\bar{1}0)$, $(\bar{1}03)$, (100), (101), respectively. [Color figure can be viewed in the online issue, which is available at wileyonlinelibrary.com.]

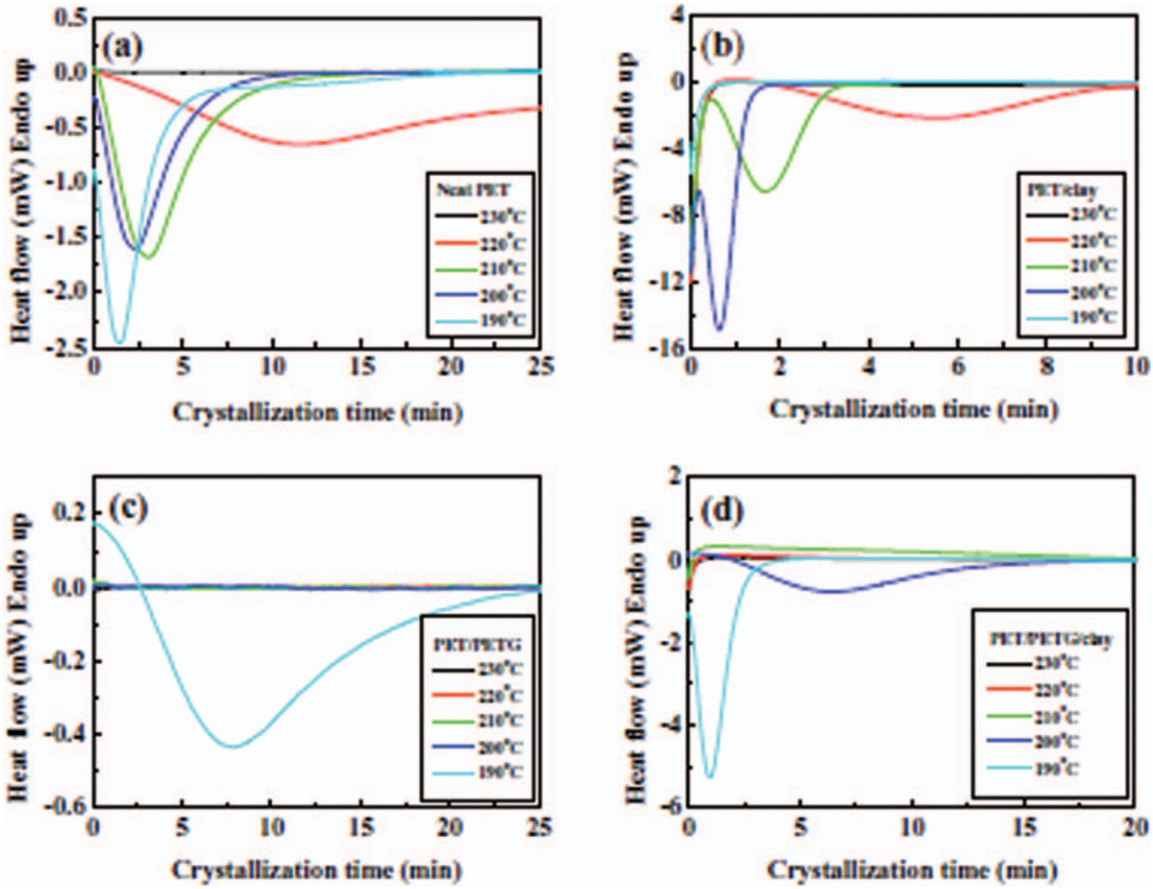

Figure 4. Isothermal crystallization DSC traces for (a) neat PET, (b) PET/clay, (c) PET/PETG, and (d) PET/PETG/clay composites at temperatures between 190 and 230°C. [Color figure can be viewed in the online issue, which is available at wileyonlinelibrary.com.]

PETG polymer. As shown in Figure 4, we studied the nominal temperature span of isothermal crystallization, in which the shape of the DSC traces could be possibly in bowl-shape, on neat PET and its composites over a 40° temperature span. It was found that this nominal temperature span is quite narrow for PET and its composites. Therefore, we conducted the investigation of isothermal crystallization for PET and its composites over 10° temperature span.

Figure 5 presents the isothermal crystallization DSC traces for neat PET, PET/clay, PET/PETG, and PET/PETG/clay at the predetermined temperatures. The crystallization enthalpies (ΔH_c) and peak crystallization times (τ_p) of neat PET and its composites can be estimated. The absolute crystallinities of neat PET and its composites can be also estimated by relating the heat of fusion of an infinitely thick PET crystal, ΔH_f^o:[24,25]

$$X_c = \frac{\Delta H_c}{\Delta H_f^o W_{\text{polymer}}} \times 100, \quad (1)$$

where ΔH_f^o is ~117.6 J/g,[23] and W_{polymer} is the weight fraction of the polymer matrix. The absolute crystallinity of PET/PETG blend can also be estimated as follows:

$$X_c = X_c' W_{\text{PET}} + X_c''(1 - W_{\text{PET}}) \quad (2)$$

where X_C' and X_C'' are the degrees of PET and PETG, respectively.

We use peak crystallization time (τ_p) to define the time taken from the onset to a point where the exothermic peak appears under isothermal crystallization. If the peak profile of crystallization is symmetric, the peak crystallization time would be exactly the same as the crystallization half-life time.[26] To possibly eliminate the deviation from DSC sample with different domain sizes, the crystallization parameters for each specimen in Table II were evaluated from four times of DSC measurement. As shown in Table II, the inclusion of amorphous PETG into the PET matrix might be responsible for the decreases in both X_c and T_m, with a simultaneous increase in τ_p for the PET/PETG blend, as compared with those values of neat PET polymer. The inclusion of clay into PET/PETG would lead to increases in both X_c and T_m, with a simultaneous decrease in τ_p for the PET/PETG/clay nanocomposite at all the predetermined crystallization temperatures, compared with those of PET/PETG counterpart. The crystallinity increment from PET/PETG to PET/PETG/clay at 195°C (15.8% vs. 16.1%) is therefore roughly 1.9%, which is significantly less than the 7.8% increment between PET at and PET/clay at 215°C (41.1% vs. 44.3%). This implies that the PETG would possibly lower the effect of heterogeneous nucleation, which is initiated by clay. Accordingly, the

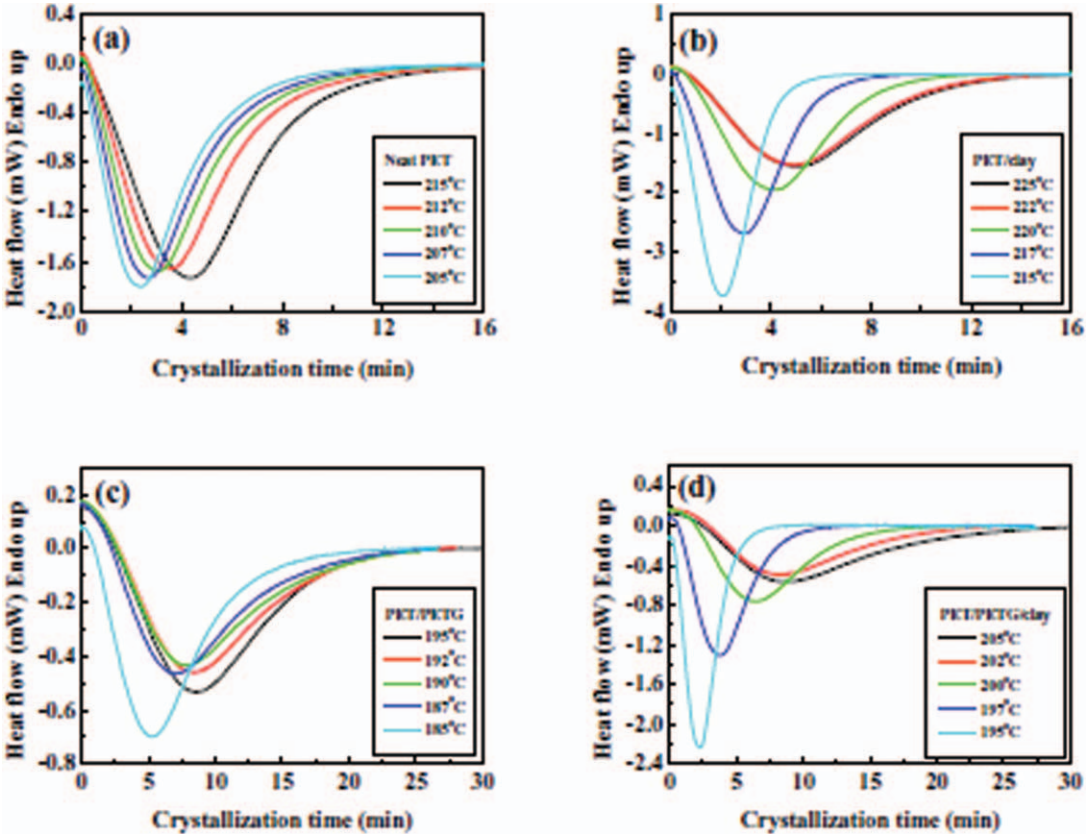

Figure 5. The isothermal crystallization DSC traces for (a) neat PET, (b) PET/clay, (c) PET/PETG, and (d) PET/PETG/clay composites at the predetermined temperatures. [Color figure can be viewed in the online issue, which is available at wileyonlinelibrary.com.]

PETG plays the opposite effect during heterogeneous nucleation, but the clay takes a role of positive effect. The inclusion of inorganic fillers is well known to affect the crystallization behavior of polymer molecules in two ways: (1) increases crystallinity and melting temperature via heterogeneous nucleation; or (2) decreases crystallinity via mobility hindrance. Our study indicated that clay may increase crystallinity and melting temperature, while the amorphous PETG decreases crystallinity via mobility hindrance.

The introduction of clay would increase the nominal crystallization temperature of PET/clay by approximately 10°C, as compared with that of neat PET. As a result, the required supercooled temperature span ΔT ($\Delta T = T_m - T_c$, where T_c is the predetermined crystallization temperature) for PET/clay is less than that of neat PET, indicating that the inclusion of clay would be easier to initiate the crystallization process of PET molecules. The same phenomenon is found in the PET/PETG/clay nanocomposite.

Isothermal Crystallization Kinetics

The Avrami equation can adequately describe the isothermal crystallization behavior, as follows:[27]

$$1 - X_c(t) = \exp(-Kt^n), \tag{3}$$

$$\ln[-\ln(1 - X_c(t))] = n \ln t + \ln K. \tag{4}$$

A plot of $\ln[-\ln(1 - X_c(t))]$ versus $\ln t$ yields the slope n, the Avrami exponent, and the intercept $\ln K$, as shown in Figure 6. Both the parameters of K and n are diagnostic of the crystallization mechanism.[27] To estimate the Avrami exponents n_1 and n_2 for the primary and secondary crystallizations, respectively, we conducted the linear fittings of $\ln[-\ln(1 - X_c(t))]$ from -4.60 to 0 for n_1 and 0 to 1.53 for n_2, corresponding to X_c equaling 0.01∼0.63 and 0.63∼0.99, respectively. In the primary crystallization stage, all the correlation coefficients (R^2) are more than 0.999, indicating a good linear fitting. As expected, the spherulites of PET polymer impinge together when the crystallinity is more than 0.75, and this range can be associated with the secondary crystallization stage. Table III shows the kinetics parameters of neat PET, PET/cay, PET/PETG, and PET/PETG/clay composites. The Avrami exponent n_1 values for neat PET and PET/clay range from 2.58–2.97 and 2.46–2.63, respectively. The inclusion of organoclay into neat PET lowered the n_1 value by 0.51 at the same crystallization temperature of 215°C, suggesting that the organoclay drives the crystal growth from dominantly three-dimensional (3D) propagation for neat PET to a combination of 3D and 2D propagation for PET/clay.

The Avrami exponent n_2 values for the secondary crystallization are also shown in Table III, and these values range from 1.97–2.39 and 1.90–2.20 for neat PET and PET/clay, respectively, which are lower than the n_1 values of neat PET by 0.58–0.61 and of PET/clay by 0.43–0.56. The crystal growth at the secondary stage of crystallization for both neat PET and PET/clay is dominantly in 2D propagation; otherwise, the crystal growth in

Table II. The Melting Temperatures (T_m), Supercooled Temperature Span ΔT ($\Delta T = T_m - T_c$), Crystallization Enthalpies (ΔH_c), Absolute Crystallinities (X_c), and Peak Crystallization Times (τ_p) of the Neat PET, PET/Clay, PET/PETG, and PET/PETG/Clay Composites Crystallized Isothermally at the Predetermined Temperatures

Sample	Crystallization temperature (°C)	T_m[a] (°C)	ΔT (°C)	$-\Delta H_c$ (J/g)	X_c[b] (%)	τ_p[c] (min)
PET	205	245.3	40.3	31.25	26.6	2.37
	207	246.7	39.7	33.96	28.9	2.67
	210	247.7	37.7	37.00	31.5	3.07
	212	248.8	36.8	40.86	34.7	3.53
	215	249.9	34.9	48.34	41.1	4.36
PET/clay	215	247.6	32.6	49.11	44.3	2.10
	217	248.3	31.3	51.72	46.6	2.94
	220	249.2	29.2	52.44	47.3	4.16
	222	250.3	28.3	52.80	47.6	4.91
	225	251.8	26.8	54.81	49.4	5.03
PET/PETG	185	223.1	38.1	36.51	15.5	5.29
	187	224.5	37.5	36.63	15.6	7.06
	190	225.8	35.8	36.84	15.7	7.90
	192	227.1	35.1	36.96	15.7	8.42
	195	229.0	34.0	37.14	15.8	8.66
PET/PETG/clay	195	227.0	32.0	35.65	16.1	2.30
	197	228.1	31.1	38.70	17.5	3.80
	200	229.2	29.2	39.69	17.9	6.55
	202	230.8	28.8	40.47	18.3	8.34
	205	233.0	28.0	41.75	18.8	8.96

[a]Standard deviation ± 1°C, [b]Standard deviation ± 3%, [c]Standard deviation 0.5 min.

primary stage for neat PET is dominantly in 3D propagation. However, the inclusion of organoclay seemly decreases the difference between n_1 and n_2 for PET/clay nanocomposite because of the higher nominal temperature of crystallization.

Figure 7 shows the morphologies of neat PET and PET/clay nanocomposite. The neat PET, which crystallized at 215°C for one minute, revealed well-defined and more perfectly spherulitic structure compared to those of PET/clay at 225°C. The completely spherulitic structure in PET seemingly occurs more frequently and evidently than in the PET/clay composite; this is consistent with the n_1 values discussed earlier. The n_1 values for neat PET are higher than those of the PET/clay nanocomposite. However, the spherulite dimensions for neat PET and PET/clay nanocomposite are approximately 5–6 and 8–10 μm, respectively. The larger spherulite dimension for PET/clay is because of the higher crystallization temperature. The growth rate K is well known to decrease with increasing crystallization temperature. In our study, the K values of PET/clay nanocomposite were still higher than those of neat PET at the same crystallization temperature (215°C). However, the K values for PET/clay crystallized at the temperature higher than 220°C decreased pronouncedly, the narrowly nominal temperature span and the less supercooled temperature span for PET/clay could be responsible for this pronounced decrease. As stated previously, both the crystallinity and melting temperature for the PET/clay nanocomposite are higher than those of neat PET. So PET/clay would have higher X_c, T_m, and K, but lower τ_p. The event of heterogeneous nucleation could seemingly be dominant in PET/clay nanocomposites during the isothermal crystallization process.

The n_1 values for the PET/PETG blend, which crystallized at a lower temperature than neat PET polymer, range from 2.41 to 2.61, which are lower than those of neat PET (2.58–2.97). The inclusion of PETG greatly reduces and dilutes the fraction percentage of crystallizable units of PET in the PET/PETG blend. Based on this postulate, the PET molecules in the PET/PETG blend should have more possibility to form larger but fewer crystallites. Moreover, the n_1 values of PET/PETG blend are lower than those of PET/clay composites (2.46–2.63). Two possibilities may account for the lower n_1 value in PET/PETG blend. One is the lower predetermined temperature for this blend, and the other is the hindrance effect because of the inclusion of PETG, which is intrinsically amorphous. The n_1 values for homogeneous and heterogeneous nucleation are well known to be 4, $(n_1 + 1)$, and 3, respectively, for 3D sphere-like crystallites; and 3 and 2, respectively, for 2D disc-like crystallites.[27] Accordingly, the geometry of crystallites for neat PET and PET/clay may appear to be possibly associated with the 3D sphere-like crystallites of the heterogeneous nucleation process. However, the PET/PETG blend may potentially display 2D disc-like crystallization.

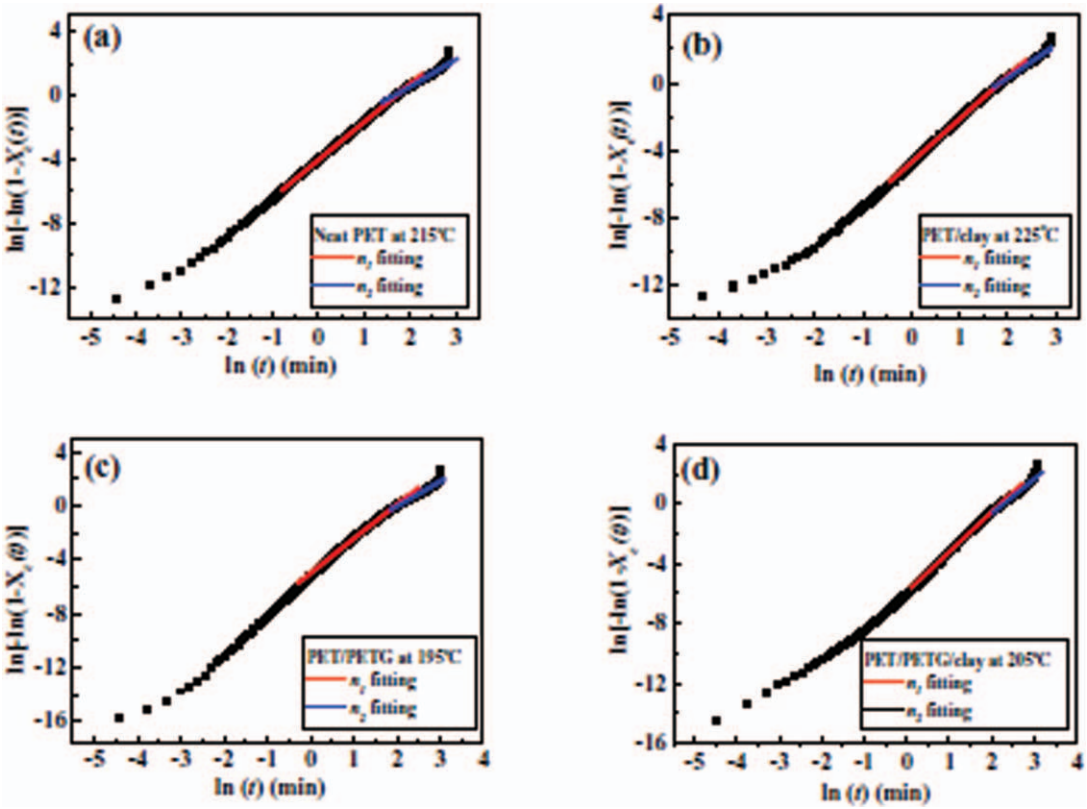

Figure 6. Plots of log[−ln(1 − $X_c(t)$)] vs. log t for (a) neat PET, (b) PET/clay, (c) PET/PETG, and (d) PET/PETG/clay composites crystallized at 215, 225, 195, and 205°C, respectively. [Color figure can be viewed in the online issue, which is available at wileyonlinelibrary.com.]

Table III. Isothermal Crystallization Kinetic Parameters of PET, PET/Clay, PET/PETG, and PET/PETG/Clay at the Predetermined Temperatures

Sample	Crystallization temperature (°C)	n_1	$K_1 \times 10^3$ ($min^{1/n}$)	n_2	$t_{1/2}$ (min)
PET	205	2.58	65.01	1.97	2.50
	207	2.66	50.72	2.03	2.67
	210	2.76	35.83	2.13	2.93
	212	2.86	24.39	2.25	3.22
	215	2.97	17.64	2.39	3.44
PET/clay	215	2.46	97.49	1.90	2.22
	217	2.55	48.64	1.94	2.83
	220	2.59	21.20	2.01	3.84
	222	2.61	9.37	2.12	5.20
	225	2.63	9.12	2.20	5.40
PET/PETG	185	2.41	5.33	1.70	7.54
	187	2.51	3.96	1.75	7.83
	190	2.56	3.23	1.86	8.14
	192	2.59	2.86	1.93	8.33
	195	2.61	2.51	1.98	8.62
PET/PETG/clay	195	2.24	30.81	1.51	4.01
	197	2.29	18.89	1.58	4.82
	200	2.32	12.82	1.61	5.58
	202	2.35	5.97	1.66	7.56
	205	2.37	5.24	1.73	7.85

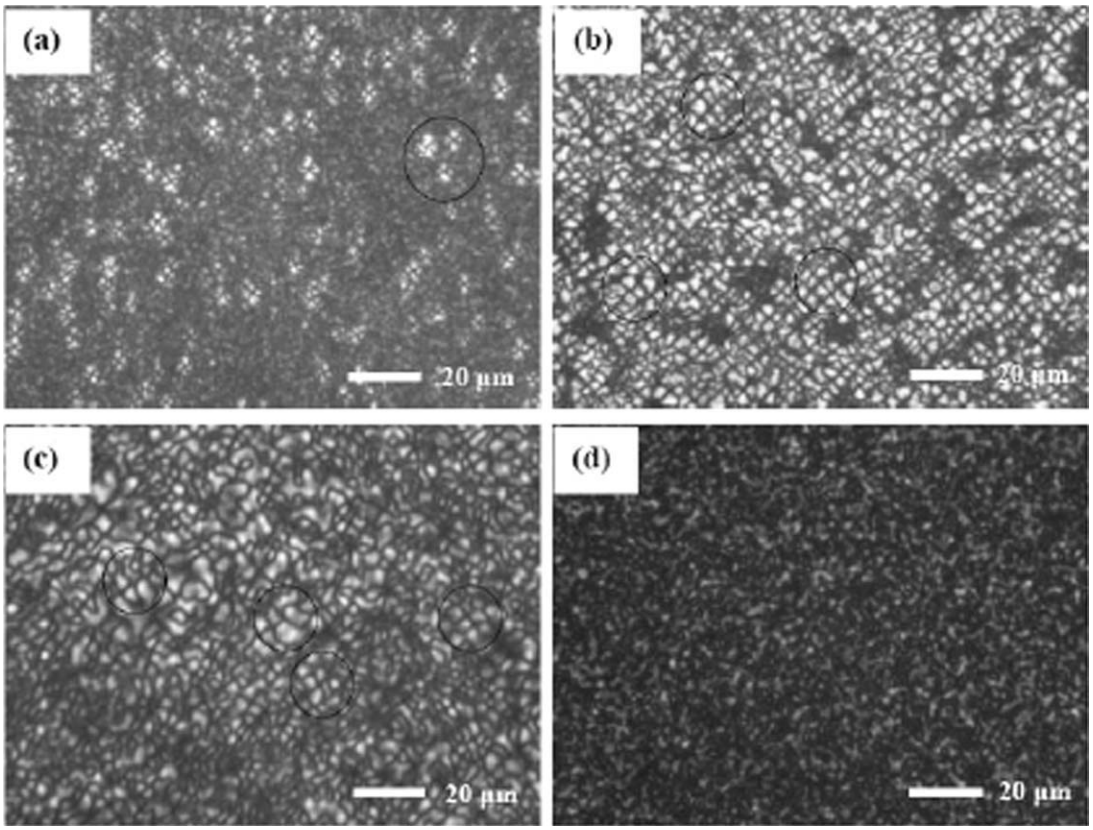

Figure 7. The spherulite morphologies of (a) neat PET, (b) PET/clay, (c) PET/PETG, and (d) PET/PETG/clay at 215, 225, 195, and 205°C, respectively, for 60 s. The circled in the pictures are the spherulite morphology of PET polymer.

Regarding the n_2 values of PET/PETG and PET/PETG/clay, these values are lower than the n_1 values of PET/PETG by 0.63–0.71 and of PET/PETG/clay by 0.54–0.63. The crystal growth at the secondary stage of crystallization for both PET/PETG and PET/PETG/clay is completely in 2D propagation, suggesting that blending PET with amorphous PETG seemly hinders the molecular diffusion during crystallization process. Also, as the event happened in PET/clay, the inclusion of organoclay seemly decreases the difference between n_1 and n_2 of PET/PETG/clay nanocomposite because of the higher nominal temperature of crystallization.

The morphology of the PET/PETG blend, as shown in Figure 7(c), could support this postulate. The spherulite morphologies in neat PET and PET/clay appear more frequently and well-developed than that in the PET/PETG blend. The crystallites in this blend exhibit fewer crystallizable units but larger crystallite dimensions (8–10 μm) compared with those of neat PET polymer. Moreover, the incorporation of PETG would cause the Maltese-cross pattern and the crystallite boundary of PET polymer to relatively disappear and become distorted, compared to those of neat PET and PET/clay. Based on the morphology of PET/PETG blend, we can assume that the crystallites in this blend may possibly propagate in two-dimensional disc-like crystallization and be associated with lower Avrami exponent n_1 value. Regarding the effect of the blending PET with PETG on the growth rate of crystallization, as shown in Table III, the inclusion of PETG greatly decreased the K value of the PET/PETG, as compared to the neat PET. The amorphous PETG significantly hinders the motion PET chain segments during crystallization.

The inclusion of clay into the PET matrix may possibly stimulate heterogeneous nucleation, as outlined previously. In Table III the n_1 values of PET/PETG/clay nanocomposite are substantially lower than those of the PET/PETG blend. This suggests that the crystallite dimension for PET/PETG/clay more likely approaches to the two-dimensional disc-like crystallization than PET/PETG blend. Figure 7(d) supports this conclusion. The morphology of PET/PETG/clay almost exhibits rod-like or disc-like crystallites, in which the Maltese-cross pattern has completely disappeared. As expected, this rod-like morphology is associated with lower n_1 values for the PET/PETG/clay nanocomposite.

Nucleation Parameters of the Isothermal Crystallization

The relation between the half-time of crystallization$t_{1/2}$ and the growth rate K can be expressed as follows:

$$t_{1/2} = (\ln 2/K)^{1/n_1} \tag{5}$$

where n_1 is the Avrami exponent. Table III shows the $t_{1/2}$ values for PET and its composites. The differences between τ_p and $t_{1/2}$ become minor when the crystallization temperatures of PET, PET/clay, PET/PETG, and PET/PETG/clay approach to 210, 220,

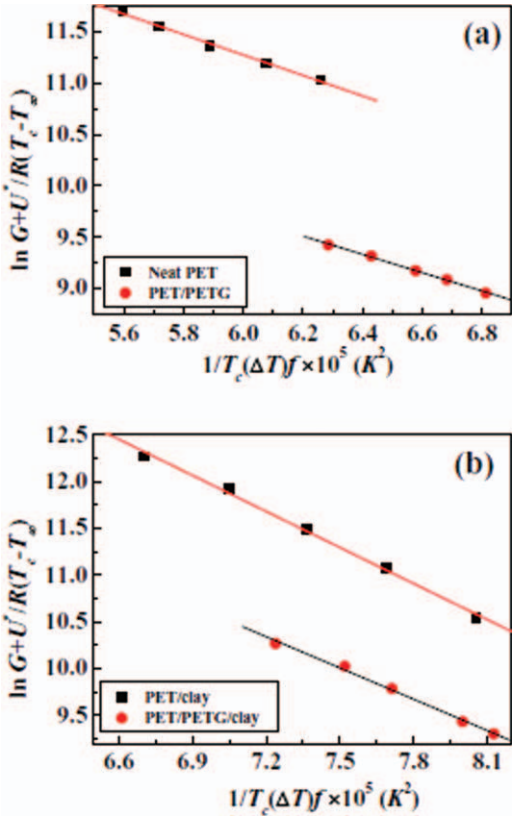

Figure 8. The Lauritzen-Hoffman plots for (a) neat PET and PET/PETG, (b) PET/clay, and PET/PETG/clay on the estimation of nucleation parameter K_g. The K_g values for neat PET, PET/clay, PET/PETG, and PET/PETG/clay are 0.99 × 10^5, 1.29 × 10^5, 0.90 × 10^5, and 1.12 × 10^5 K^2, respectively. [Color figure can be viewed in the online issue, which is available at wileyonlinelibrary.com.]

190, and 200°C, respectively, indicating that the DSC crystallization traces would tend to be more perfect in bowl-shape at theses nominal temperatures. Otherwise, the differences become significant especially in PET/PETG and PET/PETG/clay composites.

To make more in-depth insight into the crystal growth kinetics of neat PET, PET/clay, PET/PETG, and PET/PETG/clay isothermally crystallized from the melt, the secondary nucleation theory called the Lauritzen-Hoffman equation was applied to estimate the spherulitic growth rate G of the neat PET and its composites.[28] The half-time of crystallization, $t_{1/2}$, as shown in Table III, can be directly employed to describe the rate of crystallization, G, that is $G = (t_{1/2})^{-1}$.[29] As expected, the greater the value of $t_{1/2}$ leads to a lower G. At a given crystallization temperature T_c, the crystal growth rate G can be expressed by the following equation

$$G = G_o \exp\left[-\frac{U^*}{R(T_c - T_\infty)}\right] \exp\left[-\frac{K_g}{T_c(\Delta T)f}\right] \quad (6)$$

where G_o is a preexponential factor, U^* is the energy for transporting of the polymer chain segments to the crystallization site and is commonly given by a universal value of 6280 J/mol, R is the gas constant, T_∞ is a temperature below which the polymer chain movement ceases and is defined as $(T_g - C)$, where T_g is the glass transition temperature and C is a constant of 30, K_g is a nucleation parameter related to the fold and lateral surface energies, ΔT is the degree of supercooling defined as $T_m^o - T_c$, T_m^o is the equilibrium melting temperature, f is a corrective factor for the decrease of the enthalpy of fusion with the crystallization, $f = 2T_c/(T_c + T_m^o)$. There is a single T_g value for both PET and 50/50 PET/PETG blend. The T_m^o values for both PET and 50/50 PET/PETG blend are 280 and 274°C, respectively.[21] Equation (6) can be rewritten as follows:

$$\ln G + \frac{U^*}{R(T_c - T_\infty)} = \ln G_o - \frac{K_g}{T_c(\Delta T)f}. \quad (7)$$

A plot of $\ln G + U^*/R(T_c - T_\infty)$ versus $1/T_c(\Delta T)f$ yields a slope of $-K_g$, as shown in Figure 8. The K_g values for neat PET, PET/clay, PET/PETG, and PET/PETG/clay are 0.99×10^5, 1.29×10^5, 0.90×10^5, and 1.12×10^5 K^2, respectively. The nucleation parameter K_g indicates the chain mobility during nucleation process,[30] and the greater K_g value suggests the more difficulty in chain motion during nucleation. The addition of organoclay apparently retards the chain motion of PET during nucleation process. Weng et al. suggested that the inclusion of 1.5 wt % foliated graphite (FG, 50 nm in thickness) into the nylon 6 matrix lowers the chain mobility, or increases the K_g value, of nylon 6.[29] Moreover, Qiu and Yang reported that blending amorphous poly(vinyl phenol) (PVPh) with poly(butylenes succinate) (PBSU) reduces the K_g value of PBSU.[31] Our study follows the above two reports.

According to eq. (5), the greater the K_g value will result in lower value of G, i.e., a decrease in rate of crystal growth. Meanwhile, the greater ΔT as well as T_c will result in a increase in G. As shown in Table II, the inclusion of organoclay reduces the ΔT value but increases crystallization temperature T_c. However, according to eq. (6), the higher values in T_c on the organoclay filled specimens (PET/clay and PET/PETG/clay) will produce greater effect on the rate of crystal growth (G) than the values of ΔT on the neat PET and PET/PETG systems. The interaction of above three factors (K_g, ΔT, and T_c) on PET/clay nanocomposite will impart a greater G value as compared to that of neat PET, as shown in Figure 8. The G values for neat PET at 205°C, PET/clay at 215°C, PET/PETG at 185°C, and PET/PETG/clay at 195°C are 11.69, 12.27, 9.42, 10.27 μm/min, respectively. The inclusion of organoclay increases the G value of PET/clay, but blending PETG with PET decreases the G value of PET/PETG. The nylon/FG nanocomposite also shows the same trend, the G value of 1.5 wt % nylon/FG is greater than the neat nylon.[29] However, the addition of amorphous PETG to the crystallizable unit of PET reduces the G value. Qiu and Yang reported that neat PBSU shows a greater G value than the PBSU/PVPh (80/20) blend.[31]

Crystallization Activation Energy

Based on the Arrhenius model, the crystallization rate parameter K can be approximately described by the following equation:[32]

$$K^{1/n} = k_o \exp(-\Delta E/RT_c), \quad (8)$$

$$\frac{1}{n}\ln K = \ln k_o - \frac{\Delta E}{RT_c}, \quad (9)$$

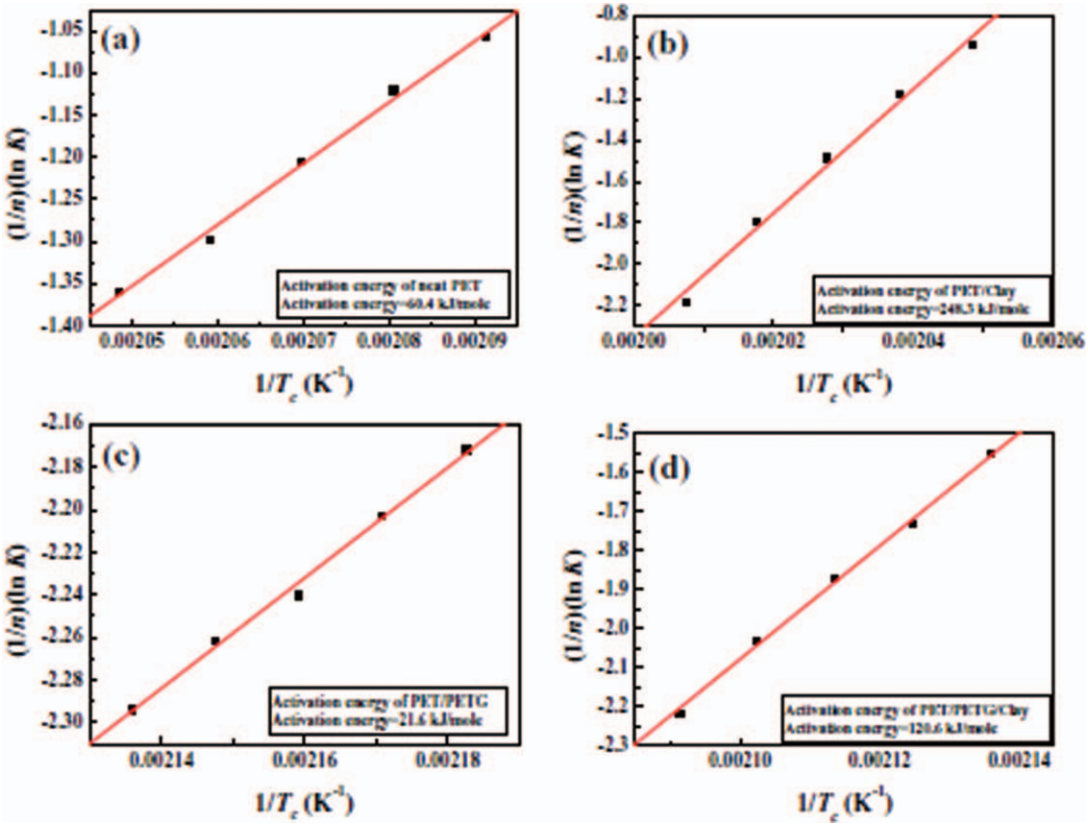

Figure 9. Activation energies for (a) neat PET, (b) PET/clay, (c) PET/PETG, and (d) PET/PETG/clay under isothermal crystallization. The values of $(-\Delta E)$ for neat PET, PET/clay, PET/PETG, and PET/PETG/clay are 60.4, 248.3, 21.6, 120.6 kJ/mole, respectively. [Color figure can be viewed in the online issue, which is available at wileyonlinelibrary.com.]

where k_o is a temperature-independent pre-exponential factor; R is the universal gas constant, and $(-\Delta E)$ is the activation energy for isothermal crystallization. Accordingly, a plot of $(1/n)\ln K$ versus $1/T_c$ provides the activation energy for the primary crystallization stage, as shown in Figure 9.

The low value of 21.6 kJ/mol for the PET/PETG blend (compared with 60.4 kJ/mol for neat PET) might be attributed to the lowest predetermined temperature among these specimens. Another factor is the lower number of crystallizable units in the blend, which may mean that the energy required for release and deposit is only one-third that of neat PET. In addition, PET/PETG/clay nanocomposite exhibits higher activation energy than that of neat PET. The inclusion of clay into the PET/PETG seems to impart more nucleating sites to this blend, which therefore necessitates releasing more energy to initiate molecular deposition.

CONCLUSIONS

On the basis of the XRD results, the inclusion of clay don't affect the crystal structure of PET polymer, and PET/PETG (50/50) blend significantly decreases the intensities at all the diffraction peaks, indicating that blending PET with PETG would suppress the crystallization behavior of neat PET polymer. Organoclay increases the crystallinity and melting temperature of PET via heterogeneous nucleation, while the amorphous PETG decreases the crystallinity and melting temperature via mobility hindrance.

The organoclay would lower the Avrami exponent n of PET, though greatly promote the growth rate K due to heterogeneous nucleation. Blending PET with PETG would decrease both n and K of PET/PETG via diffusion hindrance. The spherulites in PET/PETG blend may possibly propagate in two-dimensional disc-like crystallization and be associated with lower Avrami exponent n_1 values. The inclusion of organoclay increases the G value of PET/clay, but blending PET with PETG decreases the G value of PET. Furthermore, the inclusion of clay into PET and PET/PETG seems to introduce more nucleating sites to these matrices, and therefore, they require releasing more energy to initiate molecular deposition during crystallization process.

REFERENCES

1. Choi, W. J.; Kim, H. J.; Yoon, K. H.; Kwon, O. H.; Hwang, C. I. *J. Appl. Polym. Sci.* **2006,** *100*, 4875.
2. Zeng, K.; Bai, Y. *Mater. Lett.* **2005,** *59*, 3348.
3. Kim, S. H.; Kim, S. C. *J. Appl. Polym. Sci.* **2007,** *103*, 1262.
4. Tsai, T. Y.; Li, C. H.; Chang, C. H.; Cheng, W. H.; Hwang, C. L.; Wu, R. *J. Adv. Mater.* **2005,** *17*, 1769.
5. Hamzehlou, S. H.; Katbab, A. A. *J. Appl. Polym. Sci.* **2007,** *106*, 1375.

6. Wan, T.; Chen, L.; Chua, Y. C.; Lu, X. *J. Appl. Polym. Sci.* **2004,** *94*, 1381.
7. Calcagno, C. I. W.; Mariani, C. M.; Teixeira, S. R.; Mauler, R. S. *Polymer* **2007,** *48*, 966.
8. Wang, Y.; Shen, C.; Li, H.; Li, Q.; Chen, J. *J. Appl. Polym. Sci.* **2004,** *91*, 308.
9. Yangchuan, K.; Chengfen, L.; Zongneng, Q. *J. Appl. Polym. Sci.* **1999,** *71*, 1139.
10. Hellati, A.; Benachour, D.; Caqiao, M. E.; Boufassa, S. Calleja, F. J. *J. Appl. Polym. Sci.* **2010,** *118*, 1278.
11. Lee, S. J.; Hahm, W. G.; Kikutani, T.; Kim, B. C. *Polym. Eng. Sci.* **2009,** *49*, 317.
12. Giraldi, A. L.F.; Bizarria, M. T. M.; Silva, A. A.; Mariano, C.; Velasco, J. I.; D'Avila, M. A.; Mei, L. H. J. *J. Nanosci. Nanotechnol.* **2009,** *9*, 3883.
13. Yin, M.; Li, C.; Guan, G.; Zhang, D.; Xiao, Y. *J. Appl. Polym. Sci.* **2009,** *114*, 2327.
14. Hwang, S. Y.; Lee, W. D.; Lim, J. S.; Park, K. H.; Im, S. S. *J. Polym. Sci. Part B: Polym. Phys.* **2008,** *46*, 1022.
15. Guan, G.; Li, C.; Yuan, X.; Xiao, Y.; Liu, X.; Zhang, D. *J. Polym. Sci. Part B: Polym. Phys.* **2008,** *46*, 2380.
16. Ou, C. F.; Ho, M. T.; Lin, J. R. *J. Appl. Polym. Sci.* **2004,** *91*, 140.
17. Ou, C. F.; Ho, M. T.; Lin, J. R. *J. Polym. Res.* **2003,** *10*, 127.
18. Turner, S. R. *J. Polym. Sci. Part A: Polym. Chem.* **2004,** *42*, 5847.
19. Tsai, Y.; Fan, C. C.; Hung, C. Y.; Tsai, F. Y. *J. Appl. Polym. Sci.* **2007,** *104*, 27.
20. Tsai, Y.; Wu, J. H.; Leu, M. T. *Polym. Adv. Technol.* **2011,** *22*, 2319.
21. Papadopoulou, C. P.; Kalfoglou, N. K. *Polymer* **1997,** *38*, 631.
22. Tsai, Y.; Jheng, L.; Hung, C. Y. *Polym. Degrad. Stabil.* **2010,** *95*, 72.
23. Goschel, U. *Polymer* **1996,** *37*, 4049.
24. Anand, K. A.; Agarwal, U. S.; Joseph, R. *Polymer* **2006,** *47*, 3976.
25. Kuo, M. C.; Kuo, J. S.; Yang, M. H.; Huang, J. C. *Mater. Chem. Phys.* **2010,** *123*, 471.
26. Munehisa, Y.; Shinsuke, T.; Koji, I.; Yoshinori, O.; Yusuke, D.; Kazuhisa, T. *Polymer* **2006,** *47*, 7554.
27. Sperling, L. H. Introduction to Physical Polymer Science, 2nd ed.; Wiley: Singapore, **1993.**
28. Hoffman, J. D.; Davis, G. T.; Lauritzen, J. I. In Treatise on Solid State Chemistry; Hanny, N. B., Ed.; Plenum Press: New York, **1976;** p 7.
29. Weng, W.; Chen, G.; Wu, D. *Polymer* **2003,** *44*, 8119.
30. Wang, C.; Lin, C. C.; Tseng, L. C. *Polymer* **2006,** *47*, 390.
31. Qiu, Z.; Yang, W. *Polymer* **2006,** *47*, 6429.
32. Liu, S.; Yu, Y. N.; Cui, Y.; Zhang, H. F.; Mo, Z. S. *J. Appl. Polym. Sci.* **1998,** *70*, 2371.